MANGROVE MAPPING STRATEGIES USING GOOGLE EARTH ENGINE AND LANDSAT-8 AND SENTINEL-2 IMAGERY DATA

Flávio Henrique Rodrigues [1], Carlos Roberto de Souza Filho [1], Rebecca Del'Papa Moreira Scafutto [1], Guillaume Lassalle [1]

[1]Geosciences Institute, University of Campinas, PO Box 6152, 13083-855, Campinas, SP, Brazil.
rodrigues.ambiental@gmail.com

ABSTRACT

Vegetation indices based on remote sensing data have been widely used for mangrove monitoring. Nowadays, the availability of cloud-based platforms allows the processing of large datasets of orbital imagery with moderate spatial and spectral resolutions such as the computation of numerous vegetation spectral indices to map coastal vegetated wetlands. This study presents the performance of the Mangrove Vegetation Index (MVI) and image classification algorithms, embedded in the Google Earth Engine, applied to Landsat-8 and Sentinel-2 data, to map tracts of mangroves in Aracaju (Sergipe, Brazil). Results reveal that the Cobweb clustering algorithm applied to MVI-derived from Landsat-8 data favors reliable and practical mangrove mapping, considering the broad diversity of vegetation conditions in this habitat.

Keywords — Mangrove mapping, Google Earth Engine.

1. INTRODUCTION

Despite the growing awareness on the relevance of coastal vegetated wetlands in the balance hydrogeologic, climate control and biodiversity protection, the mangrove habitats are increasingly threatened by the agricultural and urban expansion processes, besides the releasing of contaminating compounds from industrial and port activities. To prevent these habitats from irreversible effects of technological and economic stressors, environmental monitoring measures are required. Among them, the processing of remotely sensed data is an important management tool for different goals, such as ecosystem health assessment, evaluation of environmental sensitivity to oil spill, deforestation monitoring and others [1].

Aside from photointerpretation techniques and field survey, the most widely developed mangrove mapping methods are the supervised and unsupervised spectral classifications and the vegetation indices computation. These approaches are being improved by the emerging technologies of landcover monitoring, among which, the Google Earth Engine (GEE) is a notable free access cloud-based platform with massive volumes of data and computing resources [2].

The current paper aims to compare the results obtained from the use of Mangrove Vegetation Index [3] in the image collections of Sentinel-2 and Landsat-8 provided by GEE, to assessing their potentialities for mapping of mangrove areas. The estuary of Vaza Barris River around the Aracaju (SE), Brazil, was selected for this purpose, due to it is a large coastal wetland with 12,000 hectares, comprised by mangrove forests with black, white and red species. The site is also characterized by the impacts of the oil sector, as the oil spill occurred in 2019, the largest one on Brazilian littoral.

2. MATERIAL AND METHODS

For the image preprocessing procedures, the bands related to green, near infrared and shortwave infrared 1 were used, which are equivalent to bands 3, 5 and 6 of Landsat-8 with 30 m resolution, and bands 3, 8 (10 m) and 11 (20 m) of Sentinel-2 (Fig. 1). Inside the GEE, the preprocessing algorithms removed 94.7% and 99.9 % of cloud interference of Landsat-8 and Sentinel-2 data respectively, as well as created a historical stack by their pixel median (Landsat-8: Jan/2014-Oct/2022; Sentinel-2: July/2015-Oct/2022).
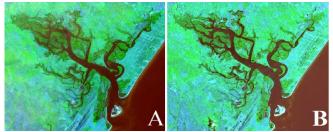

Figure 1. Compositions with bands 2, 8 and 11 of Sentinel-2 (A) and bands 2, 5 and 6 of Landsat-8 (B).

Afterward, the Mangrove Vegetation Index [3] was performed for both satellites, using the following bands:

$$MVI = \frac{NIR - Green}{SWIR1 - Green}$$

Equation 1. Mangrove Vegetation Index

The resulting MVI maps were zoned through unsupervised classification algorithms aiming at thresholding the mangrove areas. This procedure resulted in

a vector dataset, which made feasible the selection of best cluster (s) that most likely distinguish between mangrove and nom-mangrove vegetation. Subsequently, the MVI maps of both satellites were clustered by K-Means, Cascade K-Means X-Means algorithms. Learning Vector Quantization (LVQ) and Cobweb algorithms were also held, the latter one due resulting a satisfactory identification of rather broad diverse mangrove habitats such basin forests, riverine fringe threes and seaward regenerating fragments [5]. In addition, a supervised classification by the Random Forest of each satellite composition (green, NIR and SWIR1 bands) was carried out, with the aim of driving the accuracy assessment. The sample points were generated by interpretation of the high-resolution imagery of Google Earth Pro, using as reference the preliminary results from unsupervised classifications.

3. RESULTS

The supervised classification by Random Forest of Sentinel-2 and Landsat-8 imageries delimitated the mangrove areas of 56.1 and 62.2 km^2, respectively (Fig.2, A, B). This difference is resulted of a relatively greater connectivity of the mangrove fragments mapped in the Landsat-8 imagery with larger pixel size, especially at inlandward zones. Also, the indented edge of fringe mangrove fragments was further detailly flagged in the Sentinel-2 data, at tree level. The clustered maps derived from MVI performed differently for each satellite data with two main trends of mangrove delimitation: i) most clusters addressed exclusively the mangrove vegetation, segmenting it into different domains according to the water supply by the tide and river apport (Fig.2 D, I, J, L); ii) the mangrove was partially represented by one or two clusters and the others included in different spectral signature classes (Fig.2 C, E - H, K).

The visual inconsistencies are more noticeable in clustered maps with Sentinel-2 data. These maps occasionally considered as mangrove different vegetal species, especially the adjoining freshwater swamps and bushes along the sand ridges in the shoreline and hinterland. (Fig. 2, C, E, F) In some cases, the mudflats along the riverbanks and tide pools were also mapped as mangrove together with the waterbodies (Fig. 2, G, H, K). Thus, taking the supervised classified maps as reference (Fig.2 A, B), the overall accuracy and Kappa indices of MVI clustering with Sentinel-2 data ranged relatively greater than those of Landsat-8 (Table 1).

Unsupervised classification algorithms	Landsat-8		Sentinel-2	
	OA	Kappa	OA	Kappa
Cascade K-Means	0.82	0.15	0.86	0.19
K-Means	0.80	0.15	0.77	0.03
X-Means	0.83	0.11	0.86	0.18
Cobweb	0.82	0.29	0.87	0.25
LVQ	0.79	0.16	0.86	0.17

Table 1. Overall accuracy and Kappa indices of clustered MVI maps in relation to the Random Forest classification.
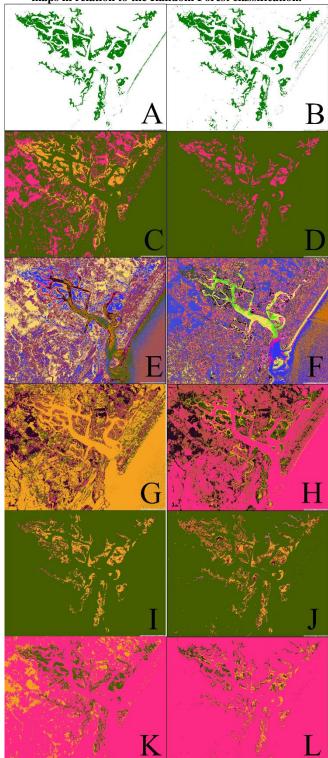

Figure 2. Random Forest classification of Sentinel-2 (A) and Landsat-8 (B) band compositions and the cluster segmentation

by Cascade K-Means, K-Means, X-Means, Cobweb and LVQ of MVI maps with Sentinel-2 (C, E, G, I, K) and Landsat-8 (D, F, H, J, L) data.

4. DISCUSSION

On the Random Forest classification, the results point out that the application of same methodological approach (equal image pre-processing procedures and spectral sample collecting) on different satellites data with similar spectral resolution, eventually leads to varied spectral assessments. This is caused by inherent aspects of the sensor dataset related to the spatial resolution and historical coverage of the site, regarding to the long-term variation of mangrove health and distribution caused by environmental stressors as climate changes, deforestation and water contamination. Moreover, the processing of cloud interference and the best pixel median had relevant influence on generation of the input data for supervised classification as well as the vegetation index computing [4]. However, despite these parameter differences, both Random Forest maps exhibited a satisfactory visual response to the diversity of estuary habitats such as the insular, riverine and brackish mangrove forests (Fig. 3).
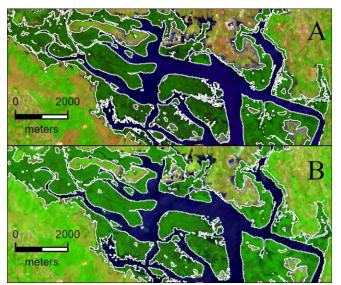

Figure 3. Detail of mangrove delimitation by Random Forest segmentation of Sentinel-2 (A) and Landsat-8 (B) imageries.

The unsupervised classification algorithms resulted a broad diversity of mangrove zoning, although the MVI suitably discriminated the spectral signature of mangrove from the other vegetation types (Fig. 4), especially for Landsat-8 with only mangrove vegetation highlighted.
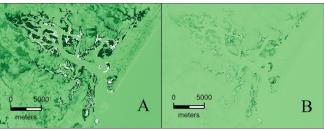

Figure 4. MVI maps from Sentinel-2 (A) and Landsat-8 (B).

In general, the accuracy assessment provided a reasonably high overall accuracy (OA) and relatively low Kappa indices for both satellites data. The incompatibility between these coefficients, more than any unconformity of the algorithms, indicates a limitation in defining the classes ("mangrove" and "non-mangrove") and selecting the training fields points for supervised classification. However, these limitations are expected, since it is exactly driven by the subjectivity of sampling of the mangrove spectral signatures, which we seek to evaluate and eventually circumvent.

The lowest OA and second lowest Kappa index for the Landsat-8 data, exhibited by the K-Means algorithm, are mainly related to the overlapped classification of mangrove fragments and adjoining vegetation along the upstream river and marshes. Two out of 15 clusters delimitated only the mangrove vegetation and a third one addressed satisfactorily the mangrove at high tide domain tough other neighboring wetland vegetations were simultaneously considered as mangrove. With lowest Kappa index and the greatest OA, X-Means produced a more conservative delimitation with only one out of five clusters dedicated to mangrove and another two misleading the mentioned adjoining habitats as mangrove, besides the hinterland, muddy areas and waterbodies. This situation reflects an area delimitation in accordance with the Random Forest map, but with a proportionally weak compatibility in the classification of mangrove and non-mangrove within these areas. The Cascade K-Means performed the best results among the K-Means methods, integrating a broader array of mangrove spectral signatures in one out of its two clusters performed.

The Sentinel-2 data also showed the lowest performance for the Cascade K-Means, X-Means and K-Means. The former two algorithms performed quite similarly with only one cluster entirely aimed at mangrove vegetation. Associated to the latter algorithm which presented two out of 15 clusters dedicated to mangrove, the lowest Kappa index and OA across all clustered MVI maps are result of the gathering of fringe and upstream mangroves in the same classes of hinterland and costal vegetation species and bared sandy soil.

The LVQ was the most contrasting classification between both sensors data, as pointed out by the divergent OA and maps (Table1; Fig.2 K, L), despite the relatively similar Kappa indices. With the Sentinel-2 data, the LVQ performed similarly to the Cascade K-Means, with only one out of four clusters exclusively aimed at mangrove zoning

and another two misleading this habitat with all sorts of spectral signature classes. Conversely, a conservative approach was observed in the Landsat-8 data exhibiting a more precise delimitation of interest areas with four out of five clusters exclusively discriminating mangrove domains. In this gradient zonation, the spatial arrangement of clusters reveals a distribution pattern of mangrove conditioned to the saline water input in the estuary as well as the tide influence on the daily water deficit of vegetation [4; 6] (Fig. 5 A).

The clustering of MVI maps by Cobweb algorithm resulted in the best mangrove delimitations for both satellites, either in visual terms or accuracy assessment (Table1; Fig.2 I, J). With the highest Kappa indices, this classifier resulted in a proper recognition of "true mangrove", reinforcing its compatibility with the supervised classification, especially for the Landsat-8. The outperformance of these satellite data is expressed by the most detailed zonation of mangrove domains with five out of six cluster exclusively designed for this purpose (Fig. 5 B). However, minor misclassifications occurred between upstream mangrove fragments and contiguous vegetated wetlands, whilst the map derived from Sentinel-2 data better deal with this issue to the detriment of most inlandward mangrove delimitation. Besides, tough its evident reliability for mangrove mapping, the MVI-Cobweb with Landsat-8 imagery still presents limitation in the recognition of outermost layers of fringe mangrove in comparison to Sentinel-2. This discrepancy may be observed in the riverine mangrove fragments illustrated in Figure 5 where the Random Forest polygons are more filled in the Sentinel-2 map (Fig. 5 C). The highest OA of this sensor data, with 87% precision, further evinces the potentiality of combined method of MVI and Cobweb using the Sentinel-2 data.
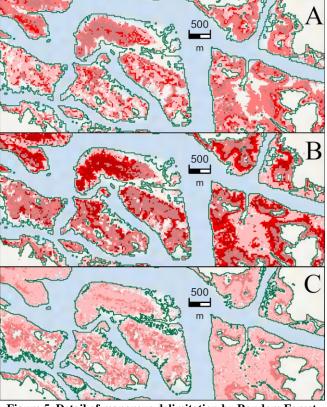

Figure 5. Detail of mangrove delimitation by Random Forest (hollow polygon with green lines) and MVI segmentation by Cobweb with Sentinel-2 (A) and Landsat-8 data (B) and by LVQ with Landsat-8 imageries (C).

5. CONCLUSION

The present comparison must not be interpreted as a definitive statement since the outputs from the preprocessing of both satellites data would significantly vary with modification of only one analysis parameters (which were currently performed at default). The aimed performance relies on the best fitting of the methods and parameters, such as the availability of data for the complete imagery preprocessing, classification algorithms supported by ground truth data and a vegetation index dedicated to the recognition of rather broad mangrove spectral signature diversity. In this regard, our study stands out the suitability of MVI computing of Landsat-8 image as a prompt and reliable mangrove mapping technique, especially when post-processed by Cobweb clustering algorithm. Therefore, further studies on the use of this combined method potentialities of Sentinel-2 data should be undertaken in order to elaborate a replicable protocol for a reliable mangrove mapping inside the Google Earth Engine, as well as other remote sensing data, preferentially available in free online repositories.

6. REFERENCES

[1] Ferreira, A. C.; Lacerda, L. D. (2016) Degradation and Conservation of Brazilian Mangroves, Status and Perspectives. *Ocean Coast. Manag*, 125, 38–46. Doi: 10.1016/j.ocecoaman.2016.03.011.

[2] Yancho, J., et al. (2020) The Google Earth Engine Mangrove Mapping Methodology (GEEMMM). *Remote Sensing*, 12 (22). doi:10.3390/rs12223758.

[3] Baloloy, A. B., et al. (2020) Development and application of a new mangrove vegetation index (MVI) for rapid and accurate mangrove mapping. *ISPRS Journal of Photogrammetry and Remote Sensing*, 166. doi:10.1016/j.isprsjprs.2020.06.001.

[4] Rogers, K., et al. (2017) Mapping of mangrove extent and zonation using high and low tide composites of Landsat data. *Hydrobiologia*, 803(1). doi:10.1007/s10750-017-3257-5.

[6] Rodrigues F. H., et al. (2023) Comparison of vegetation indices and image classification methods for mangrove mapping at semi-detailed scale in southwest of Rio de Janeiro, Brazil. *Remote Sensing Applications: Society and Environment* (Accepted article for publication).

[6] Li, W., et al. (2019) Using multi-indices approach to quantify mangrove changes over the Western Arabian Gulf along Saudi Arabia coast. *Ecol Indic*, 102, 734–745. https://doi.org/10.1016/j.ecolind.2019.03.047